JACS
JOURNAL OF THE AMERICAN CHEMICAL SOCIETY
Article
pubs.acs.org/JACS

Linear and Nonlinear Two-Coordinate Vanadium Complexes: Synthesis, Characterization, and Magnetic Properties of V(II) Amides

Jessica N. Boynton,[†] Jing-Dong Guo,[‡] James C. Fettinger,[†] Christopher E. Melton,[†] Shigeru Nagase,[‡] and Philip P. Power*[,†]

[†]Department of Chemistry, University of California—Davis, 1 Shields Avenue, Davis, California 95616, United States
[‡]Fukui Institute for Fundamental Chemistry, Kyoto University, 34-4 Takano-Nishihiraki-cho, Sakyou-ku, Kyoto 606-8103, Japan

Supporting Information

ABSTRACT: The synthesis and characterization of the first stable two-coordinate vanadium complexes are described. The vanadium(II) primary amido derivative $V\{N(H)Ar^{iPr_6}\}_2$ [Ar^{iPr_6} = C_6H_3-2,6-(C_6H_2-2,4,6-iPr_3)$_2$] (**1**) was synthesized via the reaction of $LiN(H)Ar^{iPr_6}$ with the V(III) complex $VCl_3{\cdot}2NMe_3$ or the V(II) salt $[V_2Cl_3(THF)_6]^+I^-$ in a 2:1 and 4:1 stoichiometry, respectively. Reaction of the less crowded $LiN(H)Ar^{Me_6}$ with $[V_2Cl_3(THF)_6]^+I^-$ afforded $V\{N(H)Ar^{Me_6}\}_2$ [Ar^{Me_6} = C_6H_3-2,6-(C_6H_2-2,4,6-Me_3)$_2$] (**2**), which has a nonlinear [N−V−N = 123.47(9)°] vanadium coordination. Magnetometry studies showed that $V\{N(H)Ar^{iPr_6}\}_2$ and $V\{N(H)Ar^{Me_6}\}_2$ have ambient temperature magnetic moments of 3.41 and 2.77 μ_B, respectively, which are consistent with a high-spin d^3 electron configuration. These values suggest a significant spin orbital angular momentum contribution that leads to a magnetic moment that is lower than their spin-only value of 3.87 μ_B. DFT calculations showed that the major absorptions in their UV−vis spectra were due to ligand to metal charge transfer transitions. Exposure of the reaction mixture for **2** to dry O_2 resulted in the formation of the diamagnetic V(V) oxocluster $[V\{N(H)Ar^{Me_6}\}_2]_2(\mu$-O−Li−O)$_2$ (**3**).

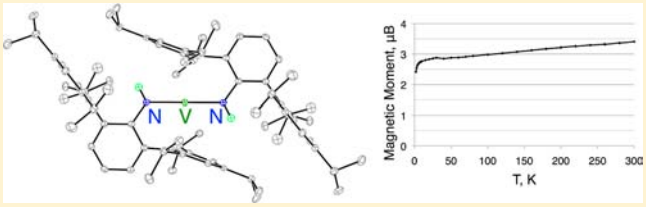

INTRODUCTION

Well-characterized, stable, two-coordinate, open-shell (d^1−d^9) transition-metal complexes are relatively rare and are confined to derivatives of the first-row metals Cr → Ni.[1,2] They are generally stabilized by using large monodentate uninegative ligands that stabilize the low coordination number by steric crowding.[1−3] Inspection of a simple d-orbital splitting diagram (see below, Figure 6)[4] of the first-row transition-metal M^{2+} ions in linear coordination shows that first-order orbital angular momentum (OAM) is expected where there are degenerate ground states as exemplified by the early transition-metal configurations d^1 (Sc^{2+}) and d^3 (V^{2+}).

Recent investigations have shown that two-coordinate, d^6 iron(II) complexes with linear or almost linear coordination display high OAM and feature essentially free ion magnetic properties.[5,6] As a result of their linear coordination, the first-order angular momentum remains essentially unquenched because the iron's ligation is solely on the *z*-axis. High magnetic moments[7,8] have also been observed in three-coordinate[9] iron(II) complexes. For the d^6 configuration of Fe^{2+}, there is a doubly degenerate orbital ground state, which is associated with the unequally occupied $d_{x^2-y^2}$ and d_{xy} orbitals. These orbitals do not interact directly with the ligands, so electron circulation is unhindered and orbital angular momentum is unquenched.[10] However, bending the coordination geometry of iron removes the ground-state degeneracy, which results in a large quenching of the OAM. In contrast, parallel work on the related d^8 configuration Ni^{2+} amide $Ni\{N(H)Ar^{iPr_6}\}_2$, which also has a degenerate ground state, has shown that its magnetic moment of 2.92 μ_B is only a little higher than the spin-only value (μ_{so} = 2.83 μ_B).[11] It was proposed that the orbital moment expected to arise from the unequally occupied d_{xz} and d_{yz} orbitals was probably quenched as a result of metal ligand π-bonding. In contrast to the iron case, the d_{xz} and d_{yz} orbitals lie at 45° with respect to the *z*-axis and so may in principle participate in such bonding, which could result in a disruption of the d-electron circulation.

Two-coordinate early transition metal complexes with d^1 or d^3 electron configurations with degenerate ground states and linear geometries are also predicted to display unquenched first-order OAM, but no stable examples of such complexes are currently known. The isolation of two-coordinate complexes of early transition metals involving σ-bonded ligands and d^1−d^3 electron configurations is more difficult than those of the later elements owing to their larger sizes and lower electron counts. These factors tend to strongly favor association and higher coordination numbers, with the result that no stable two-coordinate complexes of any of the groups 3−5 metals have been isolated.[12,13] We now report the synthesis and characterization of two two-coordinate V^{2+} (d^3) complexes that have a degenerate ground state and display magnetic properties consistent with first-order OAM. These complexes represent the first examples of stable two-coordinate vanadium derivatives and extend the known range of two-coordinate transition-metal complexes to the group 5 metals.

Received: April 1, 2013
Published: June 19, 2013

   dx.doi.org/10.1021/ja403244w | J. Am. Chem. Soc. 2013, 135, 10720−10728

Table 1. Selected Crystallographic and Data Collection Parameters for Vanadium Complexes 1−3

compd	$V\{N(H)Ar^{iPr_6}\}_2$ 2·toluene, **1**	$V\{N(H)Ar^{Me_6}\}_2$, **2**	$[V\{N(H)Ar^{Me_6}\}_2]_2$ (μ-O−Li−O)$_2$, **3**
empirical formula	$C_{86}H_{116}N_2V$	$C_{48}H_{52}N_2V$	$C_{96}H_{104}Li_2N_4O_4V_2$
formula weight (g/mol)	1228.74	707.85	1493.59
crystal system	monoclinic	triclinic	monoclinic
Space group	$C2/c$	$P\bar{1}$	$P2_1/n$
a (Å)	14.5715(7)	9.3263(4)	12.6799(6)
b (Å)	31.4168(12)	11.5802(6)	20.8049(11)
c (Å)	15.8600(6)	18.5814(8)	15.9520(8)
α (deg)	90	76.054(2)	90
β (deg)	92.9137(14)	84.829(2)	107.291(2)
γ (deg)	90	83.592(2)	90
volume (Å^3)	7251.3(5)	1931.31(16)	4018.0(4)
Z	4	2	2
density (calcd) (Mg/m^3)	1.126	1.217	1.235
absorption coeff (mm^{-1})	1.470	2.402	2.370
F(000)	2676	754	1584
crystal size (mm)	0.455 × 0.343 × 0.264	0.707 × 0.583 × 0.328	0.424 × 0.393 × 0.213
crystal color and habit	orange block	red block	orange trapezoid
θ range for data collection	2.813°−68.239°	2.455°−68.242°	8.220°−67.903°
reflections collected	25651	12749	9991
independent reflections	6422 [R(int) = 0.0340]	6723 [R(int) = 0.0188]	7200 [R(int) = 0.0394]
observed reflections [$I > 2\sigma(I)$]	6309	6547	5846
data/restraints/parameters	6422/43/469	6723/0/483	7200/0/499
goodness-of-fit on F2	1.036	1.049	1.065
final R indices [$I > 2\sigma(I)$]	R1 = 0.0412, wR2 = 0.1045	R1 = 0.0525, wR2 = 0.1548	R1 = 0.0653, wR2 = 0.1752
R indices (all data)	R1 = 0.0425, wR2 = 0.1051	R1 = 0.0533, wR2 = 0.1557	R1 = 0.0771, wR2 = 0.1832

EXPERIMENTAL SECTION

General Procedures. All manipulations were carried out under anaerobic and anhydrous conditions by using modified Schlenk line techniques under a dinitrogen atmosphere or in a Vacuum Atmospheres HE-43 drybox. All of the solvents were first dried by the method of Grubbs et al. and then stored over potassium.[14] All physical measurements were obtained under strictly anaerobic and anhydrous conditions. IR spectra were recorded as Nujol mulls between CsI or KBr plates on a Perkin-Elmer 1430 Radio recording infrared spectrometer. UV−visible spectra were recorded as dilute millimolar hexane solutions in 3.5 mL quartz cuvettes using a HP 8452 diode array spectrophotometer. Melting points were determined on a Meltemp II apparatus using glass capillaries sealed with vacuum grease and are uncorrected. Unless otherwise stated, all materials were obtained from commercial sources and used as received. $LiN(H)Ar^{Me_6}$,[15] $LiN(H)Ar^{iPr_6}$,[16] and $[V_2Cl_3(THF)_6]^+I^-$ [17] were prepared according to literature procedures.

$V[N(H)Ar^{iPr_6}]_2$ [Ar^{iPr_6} = C_6H_3-2,6-(C_6H_2-2,4,6-iPr_3)$_2$] (1). *Method A.* Approximately 25 mL of liquid NMe_3 was dried by passage as a gas through a P_2O_5 drying column and added to 0.33 g of VCl_3 (2 mmol) with cooling to ca. −78 °C. The suspension was stirred for 1 week at this temperature. To the resulting dark purple-brown slurry was added $LiN(H)Ar^{iPr_6}$ (2.0 g, 4 mmol) via a solid addition funnel. The resulting mixture was allowed to stir at ca. −78 °C for 3 days. The flask was allowed to warm to room temperature and solvent was removed under reduced pressure. The resulting orange brown solid was extracted with ca. 25 mL of hexane and filtered via cannula. The dark orange solution was concentrated to ca. 10 mL and after storage for 3 days at −18 °C afforded X-ray quality crystals of **1**. Yield: 0.56 g (27%). Mp 143 °C dec, UV−vis, nm (ε, M^{-1} cm^{-1}): 298 (19 000) and 418 (10 000). IR, Nujol mull (cm^{-1}) in CsI: ν_{N-H} 3480 (w), ν_{V-N} 555 (w). 3.41 μ_B.

Method B. A ca. 20 mL ether solution of 0.80 g (1.58 mmol) of $LiN(H)Ar^{iPr_6}$ was added dropwise via cannula to an ether solution (ca. 20 mL) of 0.29 g (0.38 mmol) of $[V_2Cl_3(THF)_6]^+I^-$ at ca. −78 °C. After warming to room temperature overnight, the resulting orange-brown solution was allowed to stir for 48 h, whereupon the solvent was removed under reduced pressure and the residue was extracted with hexane. Upon reduction of the volume to ca. 20 mL under reduced pressure the solution was stored in a ca. −18 °C freezer for 3 days to afford an orange precipitate. The mother liquor was decanted from the orange powder, which was dried under reduced pressure and redissolved in ca. 10 mL of toluene. Storage at −18 °C for 3 days afforded dark orange crystals of **1**. Yield: 0.17 g (25%).

$V[N(H)Ar^{Me_6}]_2$ [Ar^{Me_6} = C_6H_3-2,6-(C_6H_2-2,4,6-Me_3)$_2$] (2). A ca. 20 mL ether solution of 0.50 g (1.50 mmol) of $LiN(H)Ar^{Me_6}$ was added dropwise via cannula to an ether solution (ca. 20 mL) of 0.286 g (0.375 mmol) of $[V_2Cl_3(THF)_6]^+I^-$ at ca. −78 °C. Upon warming to room temperature overnight the resulting red-brown solution was allowed to stir for 48 h. The solvent was removed under reduced pressure and the residue was extracted with toluene. Reduction of the volume to ca. 20 mL under reduced pressure and storage at −18 °C for 3 days afforded **2** as a red microcrystalline powder. The powder was redissolved in ca. 25 mL of pentane and stored at ambient temperature inside a glovebox for 2 days to yield red crystals that were suitable for X-ray crystallography of **2**. Yield: 0.195 g (10%). Mp: 225−228 °C. UV−vis, nm (ε, M^{-1} cm^{-1}): 296 (450), 342 (200), 407 (150), 527 (100). IR, Nujol mull (cm^{-1}) in CsI: ν_{N-H} 3481, 3384 (w); ν_{V-N} 634(w). 2.77 μ_B. Anal. Calcd for $C_{48}H_{52}N_2V$: C, 81.44; H, 7.41; N, 3.96. Found: C, 81.73; H, 7.44; N, 4.01.

$[V\{N(H)Ar^{Me_6}\}_2]_2$(μ-O−Li−O)$_2$ (3). A ca. 20 mL ether solution of 0.50 g (1.50 mmol) of $LiN(H)Ar^{Me_6}$ was added dropwise via cannula to an ether solution (ca. 20 mL) of 0.286 g (0.375 mmol) of $[V_2Cl_3(THF)_6]^+I^-$ at ca. −78 °C . After warming to room temperature overnight the resulting red-brown solution was allowed to stir for 48 h. When the reaction was complete, two equiv of dry O_2 was added via syringe, and an immediate color change to red-orange was observed. The solvent was removed under reduced pressure and the red residue was extracted with toluene. After reducing the volume to ca. 10 mL under reduced pressure, storage at 25 °C for 1 week afforded red-orange crystals of **3**. Yield: 0.5324 g (94.9%). Mp: 105−107 °C. UV−vis, nm (ε, M^{-1} cm^{-1}): 294 (17 600). IR, Nujol mull (cm^{-1}) in KBr: ν_{N-H} 3462, 3375 (w). Diamagnetic. Anal. Calcd for $C_{48}H_{52}LiN_2O_2V$: C, 77.19; H, 7.02; N, 3.75. Found: C, 77.61; H, 6.91; N, 3.68.

X-ray Crystallography. Orange-brown, X-ray-quality crystals of **1** were obtained from a concentrated toluene solution after storage at ca. −18 °C for 3 days. Red, X-ray-quality crystals of **2** were obtained from

dx.doi.org/10.1021/ja403244w | J. Am. Chem. Soc. 2013, 135, 10720−10728

Scheme 1. Synthetic Routes to $V\{N(H)Ar^{iPr_6}\}_2$ (1), $V\{N(H)Ar^{Me_6}\}_2$ (2), and $[V\{N(H)Ar^{Me_6}\}_2]_2$ (μ-O−Li−O)$_2$ (3)

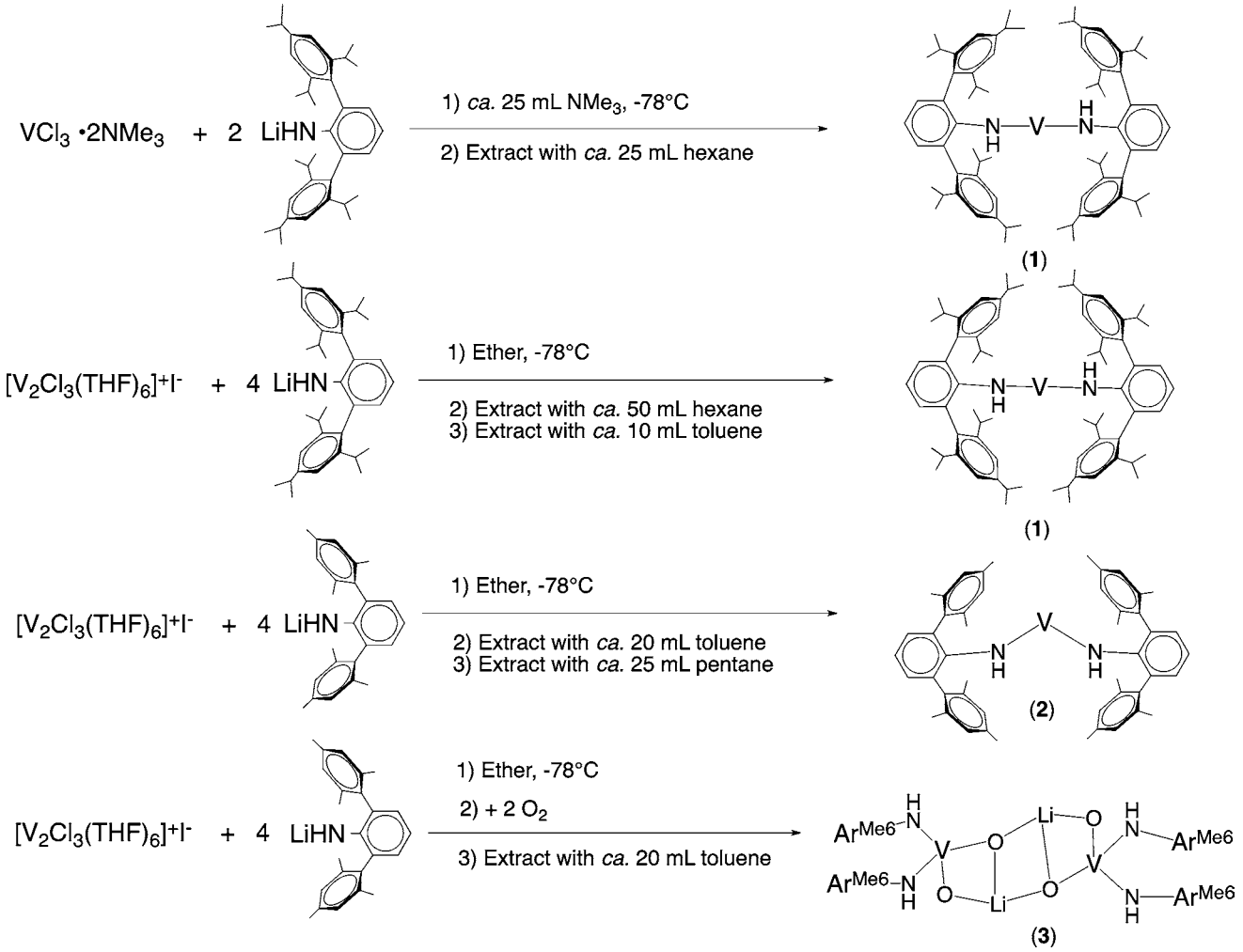

a concentrated pentane solution after storage at ca. 25 °C for 2 days. Red-orange, X-ray-quality crystals of **3** were obtained from a concentrated toluene solution after storage at ca. 25 °C for 1 week. Suitable crystals were selected and covered with a layer of hydrocarbon oil under a rapid flow of N_2. They were mounted on a glass fiber attached to a copper pin and placed in a cold N_2 stream on a diffractometer. X-ray data for **1**−**3** was collected at 90(2) K with 1.5418 Å Cu Kα_1 radiation with a Bruker DUO-APEX-II diffractometer in conjunction with a CCD detector.[18] The collected reflections were corrected for Lorentz and polarization effects and for absorption by use of Blessing's method as incorporated into the program SADABS.[19] The structures were solved by direct methods and refined with the SHELXTL v.6.1 software package.[20] Refinement was carried out by full-matrix least-squares procedures with all carbon-bound hydrogen atoms included in calculated positions and treated as riding atoms. N-Bound hydrogens were located directly from the Fourier difference map. Details of each crystal structure for **1**−**3** along with second crystal structures of **1** are located in the Supporting Information. A summary of crystallographic and data collection parameters for **1**−**3** is given in Table 1.

Magnetic Measurements. Compacted powder samples of **1** and **2** were sealed under vacuum in a 3 and 5 mm diameter quartz tube, respectively. The magnetic properties were measured using a Quantum Design MPMSXL7 superconducting quantum interference magnetometer; the sample was first zero-field cooled to 2 K and its moment was measured upon warming from 2 to 300 K in an applied field of 0.01 T. In order to ensure thermal equilibrium between the sample in the quartz tube and the temperature sensor, the moment was measured at each temperature until it reached a constant value; ca. 15 h were required for the measurements. A diamagnetic correction of −0.000775 and −0.000491 emu/mol, obtained from tables of Pascal's constants,[21] was applied to the measured molar magnetic susceptibility of **1** and **2**. Following the above study, the same sample **1** was cooled to 5 K and its magnetization was measured in a field of ±7 T; no magnetic hysteresis was observed in this study.

DFT Calculations. All calculations were carried out using the Gaussian 09 program.[22] Geometry optimization was performed with hybrid density functional theory (DFT) at the spin-unrestricted B3PW91[23,24] level for complexes **1** $[V\{N(H)Ar^{iPr_6}\}_2]$ and **2** $[V\{N(H)Ar^{Me_6}\}_2]$ using the 6-311+G* basis set for the V atom, the 6-31G(d) basis set for the N atom, and the 6-31G basis set for C and H atoms. On the basis of the optimized geometries, the unscaled vibrational frequencies and the UV/vis absorption wavelengths estimated by the time-dependent DFT (TD-DFT) method were obtained with the B3PW91 method.

RESULTS AND DISCUSSION

Synthesis. Compound **1** was synthesized by two separate synthetic methods. Preliminary experiments involving the reaction of the lithium amide with the readily available V(III) halide precursor $VCl_3(THF)_3$[25] as the vanadium source were unsuccessful. We found that the use of VCl_3 suspended in trimethylamine[26a] gave modest but reproducible yields of **1**. Disproportionation[26b] of the V(III) salt apparently occurred, and compound **1** was formed as shown in Scheme 1. A more rational synthesis of compound **1** was accomplished via simple salt elimination involving the V(II) halide precursor $[V_2Cl_3(THF)_6]^+I^-$. Treatment of the salt with 4 equiv of $LiN(H)Ar^{iPr_6}$ in ether solution gave

dx.doi.org/10.1021/ja403244w | J. Am. Chem. Soc. 2013, 135, 10720−10728

reproducible yields of $V\{N(H)Ar^{iPr_6}\}_2$ (**1**). The same approach was then used for compound **2**, in which treatment of the $[V_2Cl_3(THF)_6]^+I^-$ salt with 4 equiv of $LiN(H)Ar^{Me_6}$ gave consistent yields of $V\{N(H)Ar^{Me_6}\}_2$ (**2**). The synthetic routes to **1** and **2** differ from the approach used for the analogous iron complex,[6] which was obtained by treatment of $Fe\{N(SiMe_3)_2\}_2$[27] with 2 equiv of the primary amine. A transamination approach was also attempted for vanadium in the synthesis of compound **1** by treating $V\{N(SiMe_3)_2\}_3$[28] with 2 equiv of the primary amine, but no reaction was observed under ambient conditions and with heating. The addition of dry O_2 to a solution of **2** led to the oxidation of V(II) to V(V) and the coordination of two bridging lithium counter cations. Attempts to synthesize **3** by the addition of KO_2 to **2** were unsuccessful. Reactions of **1** with O_2, ethylene, and ^{t}BuOO^{t}Bu in the absence of LiCl yielded intractable products.

Structures. The structure of **1** is shown in Figure 1, and selected bond lengths and angles are given in Table 2. The

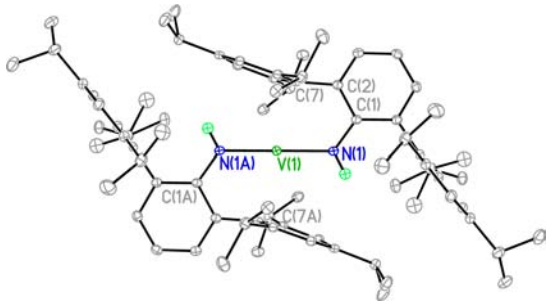

Figure 1. Thermal ellipsoid (30%) drawing of the linear two-coordinate $V\{N(H)Ar^{iPr_6}\}_2$ (**1**). Non-nitrogen H atoms are not shown for clarity. Select bond distances and angles are given in Table 2.

structure of **2** is illustrated in Figure 2, and selected bond lengths and angles are given in Table 2. The complexes $V\{N(H)Ar^{iPr_6}\}_2$ and $V\{N(H)Ar^{Me_6}\}_2$ are the first well-characterized homoleptic vanadium(II) amides[29a] and the first examples of stable two-coordinate[2] vanadium complexes.

The more crowded complex $V\{N(H)Ar^{iPr_6}\}_2$ possesses a 2-fold rotational axis passing through the metal and almost linear coordination [N–V–N = 179.98(7)°]. The ipso carbons of the

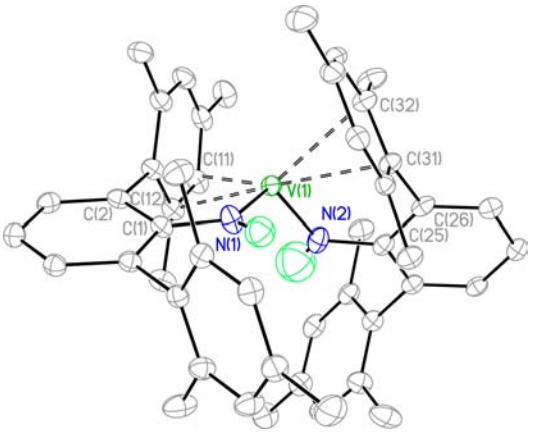

Figure 2. Thermal ellipsoid (30%) drawing of the nonlinear two-coordinated $V\{N(H)Ar^{Me_6}\}_2$ (**2**). Non-nitrogen H atoms are not shown for clarity. Selected bond distances and angles are given in Table 2. Another structure of **2** showing the second vanadium site is shown in the Supporting Information.

central aryl rings of the terphenyl group, the nitrogens, the hydrogens on the two nitrogens, and vanadium form an almost planar array with the terphenyls disposed in a trans fashion, resulting in roughly local C_{2h} symmetry for the $M\{N(H)C(ipso)\}_2$ moiety. The M–N bonds are both 1.9916(12) Å long, which is a similar distance to those found in the analogous chromium complex and is consistent with the almost identical Shannon–Prewitt radii for the V^{2+} (0.93 Å) and Cr^{2+} (0.94 Å) of these ions in octahedral coordination.[30a] A second X-ray data set (see Supporting Information) for a crystal of **1** obtained from hexane afforded a molecule with very similar structure with no imposed symmetry and features a V–N distance of 1.9948(12) Å and an N–V–N angle of 178.68(5)° that are essentially indistinguishable from those given above. In agreement with the similar ionic radii of V^{2+} and Cr^{2+}, both V–N bond lengths are indistinguishable from the 1.9966(14) Å observed in $Cr\{N(H)Ar^{iPr_6}\}_2$.[30b] The V–N bond length, with consideration of the standard deviation, is also the same as the V–N distance reported recently [2.000(2) Å] for the three-coordinate V(II)

Table 2. Selected Interatomic Distances (Å) and Angles (deg) for the Complexes 1–3

	$V\{N(H)Ar^{iPr_6}\}_2$ (**1**)	$V\{N(H)Ar^{Me_6}\}_2$ (**2**)	$[V\{N(H)Ar^{Me_6}\}_2]_2(\mu$-O–Li–O$)_2$ (**3**)
V–N(1)	1.9916(12)	1.976(2)	1.902(2)
V–N(2)		1.936(2)	1.907(2)
V––C(aryl)	2.5330(13)	2.605(2)	
V––C(11)		2.463(2)	
V––C(12)		2.521(2)	
V––C(31)		2.487(2)	
V––C(32)		2.557(2)	
N(1)–V–N(1a/2)	179.98(7)	123.47(9)	114.55(10)
V–N(1)/N(2)–(H)	117.4/117.4	117.7/117.9	108.1/107.8
V–N(1)–C(1)	125.29(9)	124.51(14)	143.78(19)
V–N(2)–C(27/37)	125.29(9)	105.00(15)	144.38(19)
V(1)–O(1)			1.6307(19)
V(1)–O(2a)			1.6462(19)
O(1)–V(1)–O(2a)			104.13(9)
N(1)–V(1)–O(1)			108.76(10)
N(2)–V(1)–O(2a)			103.43(10)
Li(1)–O(2)			1.840(6)
Li(1)–O(1)			1.938(6)
Li(1)–O(2a)			2.258(6)

dx.doi.org/10.1021/ja403244w | J. Am. Chem. Soc. 2013, 135, 10720–10728

derivative $(HC\{C(Me)NDipp\}_2)V(ODipp)$[31] (Dipp = C_6H_3-2,6-*i*Pr_2). It can be seen that the two flanking aryl rings are bent away from the vanadium and feature a C(2)−C(7)−C(10) angle of 15.19°, apparently because of the steric repulsion of the *p*-isopropyl groups, although dispersion forces between the *o*-*i*Pr groups are also probably present. The shortest V−C distance to the flanking aryl ring is V−C(7) at 2.5330(13) Å (V-centroid = 2.94 Å), which is considerably longer than the ca. 2.09 Å that would be expected for a V−C single bond.[32] Bond distances and angles predicted by DFT calculations on the full molecule (Table 3) are consistent with experimental data.

Table 3. DFT Calculated Select Bond Distances (Å) and Angles (deg) for Complexes 1 and 2

	V{N(H)Ar^{iPr_6}}$_2$ (**1**)		V{N(H)Ar^{Me_6}}$_2$ (**2**)	
	calcd B3PW91	expt	calcd B3PW91	expt
V−N	1.994	1.9916(12)	1.972	1.976(2)/1.936(2)
N−C	1.378	1.384	1.379	1.372/1.367
N−V−N	180.0	179.98(7)	141.3	123.47(9)
V−N−C	127.0	125.29(9)	125.6	124.51(14)

The existence of relatively close approaches between vanadium and carbon atoms of the flanking aryl rings of the terphenyl substituents in **1** raises the question of the "true" coordination number of the metal. Such interactions have been deemed to raise the effective metal coordination number on the basis of Mössbauer data on iron(II) thiolato species.[29a,b] However, the Mössbauer data for the iron(II) analogue of **1**, Fe{N(H)Ar^{iPr_6}}$_2$ do not support the higher coordination viewpoint.[6] Furthermore, the lack of significant quenching of the orbital angular momentum in the iron species suggests that the metal−carbon secondary interactions are weak in these linear geometry species.

The structure of V{N(H)Ar^{Me_6}}$_2$ (**2**) is shown in Figure 2 and has a strongly bent geometry with a N−V−N angle of 123.47(9)°, in contrast to the linearly coordinated V{N(H)Ar^{iPr_6}}$_2$. The vanadium is disordered over two locations, and the structure illustrated in Figure 2 features the major (80%) occupancy site.

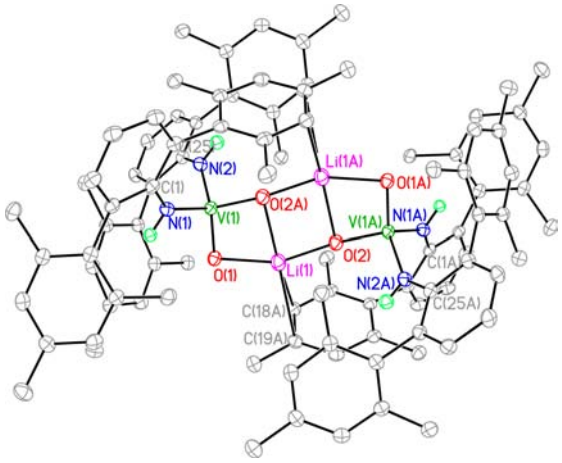

Figure 3. Thermal ellipsoid (30%) drawing of the two-coordinate $[V\{N(H)Ar^{Me_6}\}_2]_2(\mu\text{-O-Li-O})_2$ (**3**). Non-nitrogen H atoms are not shown for clarity. Select bond distances and angles are given in Table 2.

Table 4. DFT-Calculated UV−Visible Absorption Data for Complexes 1 and 2

calculated (gas phase)		experiment		
λ, nm (eV)	oscillator strength (10^{-2})	λ, nm (eV)	strength (ε, M^{-1} cm^{-1})	λ offset (eV) calcd vs expt
		V{N(H)Ar^{iPr_6}}$_2$ (**1**)		
454 (2.73)	10.85	418 (2.97)	10000	0.24
287 (4.32)	10.95	298 (4.16)	19000	0.16
		V{N(H)Ar^{Me_6}}$_2$ (**2**)		
497 (2.50)	0.57	527 (2.35)	100	−0.15
419 (2.96)	2.73	407 (3.05)	150	0.09
337 (3.68)	6.52	342 (3.63)	200	−0.05
276 (4.49)	8.55	296 (4.19)	450	−0.14

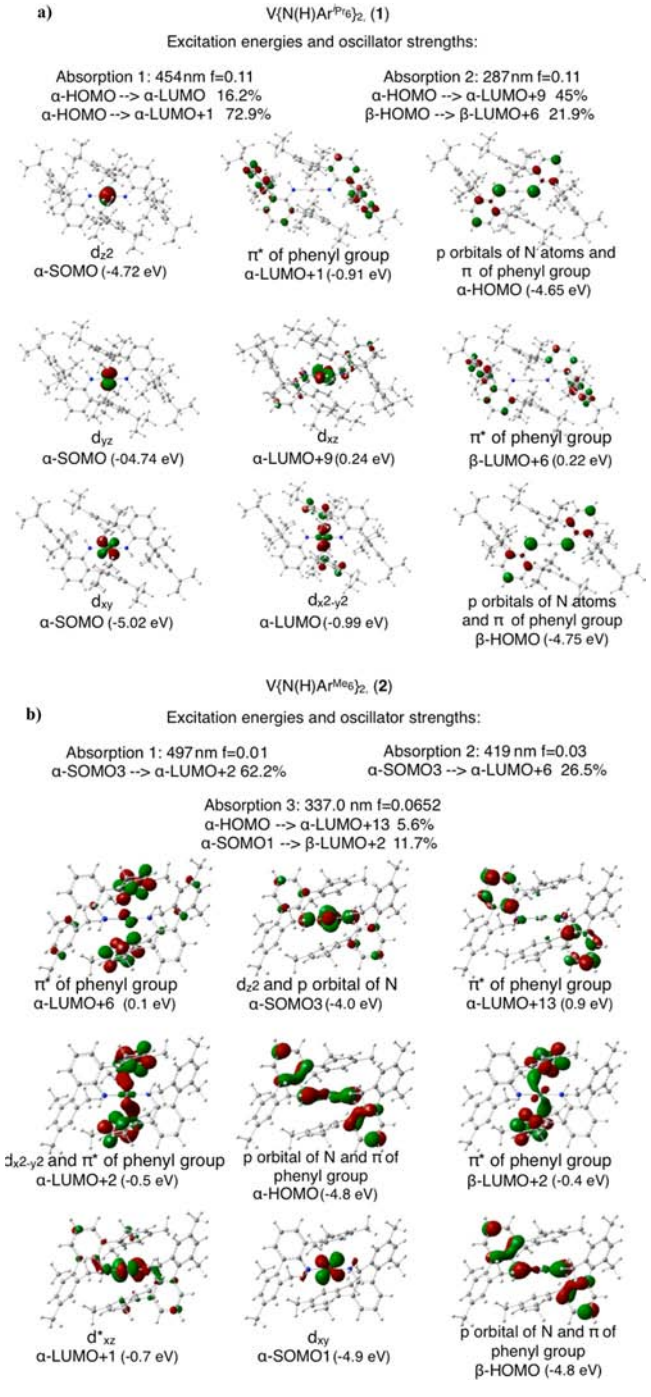

Figure 4. The DFT-calculated electronic transitions for (a) V{N(H)-Ar^{iPr_6}}$_2$ (**1**) and (b) V{N(H)Ar^{Me_6}}$_2$ (**2**).

dx.doi.org/10.1021/ja403244w | J. Am. Chem. Soc. 2013, 135, 10720−10728

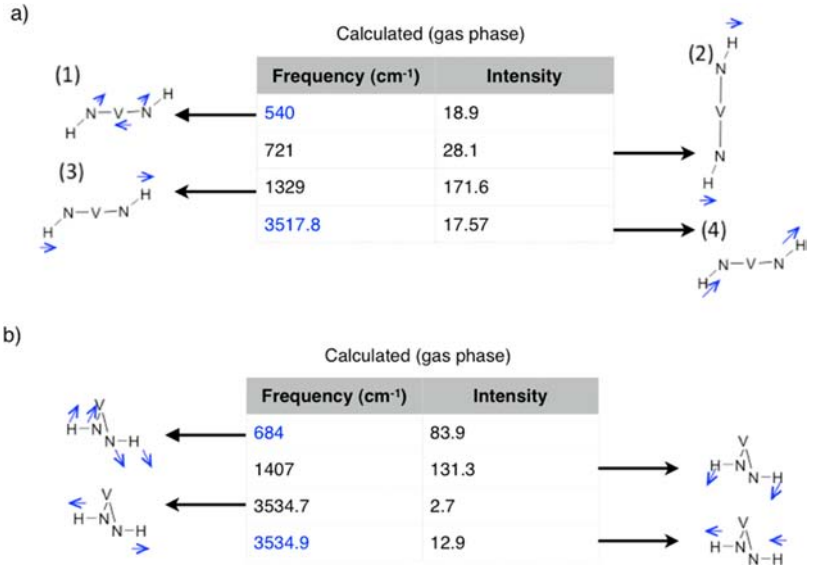

Figure 5. DFT calculated infrared spectra for (a) complex $V\{N(H)Ar^{iPr_6}\}_2$ (**1**) and (b) complex $V\{N(H)Ar^{Me_6}\}_2$ (**2**). Frequencies shaded in blue correspond to those observed experimentally.

The other vanadium site is illustrated in the Supporting Information. It involves a N−V−N angle of only 107.33(14)° and is strongly coordinated to one of the flanking aryl rings of the ligand [V−C(aryl) = 1.839 Å]. Apparently, the decreased bulk of the ligand allows the aryl rings a more flexible orientation and stronger vanadium interactions with the flanking aryl rings, where the closest V−C distances are 2.463(2) and 2.487(2) Å, and the V−centroid distances are 2.605(2) Å [C(7) ring] and 2.690(2) Å [C(31) ring]. An examination of vanadium−aryl bonding interactions shows that distances to the centroid and carbons of the ring are considerably closer in compounds such as $VInd_2$ (Ind = η^5-C_9H_7) and $[V\{\mu$-(η^6-2,6-$Me_2C_6H_3N$)C(Me)CHC(Me)C(N-2,6-$Me_2C_6H_3$)$\}]_2$ [ranging from 1.744(4) to 2.412(8) Å] than those observed in compound **2**.[33] The V−N distances in **2** at 1.976(2) and 1.936(2) Å are slightly shorter than those in **1**. This is consistent with the lower degree of crowding imposed by the ligands.

The structural parameters calculated by DFT for **1** are in very good agreement with the experimentally determined values (Table 3). In **2** the agreement between the experimentally determined N−V−N angles and the angles predicted by the B3PW91 level is not as close as that in **1** (Table 3). It is probable that the N−V−N angle in **2** is restricted by packing forces in the X-ray crystal structure because there is only 1.2 kcal/mol of the potential energy difference between the fully and partially (with only the N−V−N angle frozen at the experimental value) optimized structures at the B3PW91 level, suggesting that the energy difference between the two structures is small. Despite the N−V−N angular difference, it can be seen that the other bond distances and angles calculated for **2** are in good agreement with those experimentally determined.

Figure 3 shows the X-ray crystal structure of the compound $[V\{N(H)Ar^{Me_6}\}_2]_2(\mu$-O−Li−O$)_2$ (**3**), which is the result of the introduction of dry oxygen during the synthesis of **2** (a similar experiment in the case of **1** did not afford a crystalline metal oxo product). In this compound vanadium has been oxidized to the +5 state and its structure is characterized by the presence of a center of symmetry relating the $[V\{N(H)Ar^{Me_6}\}_2]_2(\mu$-O) units to each other by bridging Li^+ ions complexed to the oxygens. Each vanadium(V) atom has a distorted tetrahedral coordination and is bonded to two nitrogen and two oxygen atoms. The central cluster is in a laddering arrangement of Li, V, O, and N atoms, which is similar to those described previously for amidolithium compounds.[34] The O−V−O angle is 104.13(9)°, whereas the N−V−N angle is a wider 114.42(10)°, presumably due to the steric hindrance of the terphenyl substituents. The V−N distances 1.904(3) and 1.907(4) Å in **3** are significantly shorter than those observed in the V(II) compounds **1** and **2**, which is consistent with the higher charge (+5) and a smaller size of the V^{5+} ionic radius (0.495 Å) in comparison to that of V^{2+} (0.93 Å).[30a] The V−O(1/1a) and V−O(2/2a) bond lengths are 1.6307(19) and 1.6462(19) Å, consistent with VO double bonding, and are close to the ca. 1.6 Å V−O distance found in vanadyl complexes.[35] These short V−O lengths are similar to the V=O bond distances [1.605(2)−1.629(2) Å] observed in dioxo[(*S*)-*N*-salicylidene-3-aminopyrrolidine]vanadium(V)[36a] and [1.6064(10)−1.6251(15) Å] observed in VO_2(PyPzOAPz) (PyPzOAPz = *N*-[amino(pyrazin-2-yl)methylidene]-5-methyl-1-(pyridin-2-yl)-1*H*-pyrazole-3-carbohydrazonic acid).[36b] In contrast, the distances are significantly shorter than the single bond distances of 1.965(4) and 2.032(4) Å seen in the bridged species $V\{N(SiMe_3)(SiMe_2C(CH_2)O)\}_2$[37] and the terminal V−O distance of 1.836(2) Å observed recently in the three-coordinate V(II) complex $(HC\{C(Me)NDipp\}_2)V(ODipp)$,[31] indicating that both oxygens are double bonded to the vanadium metal atom.[38] The Li−O distances are Li(1)−O(2) = 1.840(6) Å, Li(1)−O(1) = 1.938(6) Å, and Li(1)−O(2)a = 2.258(6) Å, which are typical of Li−O distances in structures such as $(LiOAr^{iPr_4})_2$ [Ar^{iPr_4} = C_6H_3-2,6-(C_6H_3-2,6-iPr_2)$_2$][39] [Li−O = 1.807(3) and 1.979(3) Å] and consistent with those in the structures of lithium alkoxides that feature distances in the range of 1.825(4)−2.197(9) Å.[40] In effect, the structure of **3** may also be regarded as consisting of two bis(amido)dioxovanadium(V) monoanions connected by two bridging Li^+ cations.

Electronic Spectroscopy. The UV−visible absorption spectra of the intensely colored orange-red complexes **1**−**3** in millimolar hexane solution revealed moderately intense electronic transitions for these complexes. UV−vis absorption maxima [λ_{max}, nm (ε, M^{-1} cm^{-1})] were observed at 298 (19 000) and 418 (10 000) for the linear complex **1**. The nonlinear complex

dx.doi.org/10.1021/ja403244w | J. Am. Chem. Soc. 2013, 135, 10720−10728

2 displayed absorption maxima [λ_{max}, nm (ε, M^{-1} cm^{-1})] at 296 (450), 342 (200), 407 (150), and 527 (100). Complex **3** displayed a ligand charge-transfer absorption [λ_{max}, nm (ε, M^{-1} cm^{-1})] at 294 (17 600).

DFT calculations at the B3PW91 level for complex **1** indicated good agreement with the experimentally observed spectroscopic data (Table 4). The highest energy absorption (287 nm, 34 855 M^{-1} cm^{-1}) that was calculated (cf. observed values, 298 nm, 19 000 M^{-1} cm^{-1}) corresponds to the transition from the ligand nitrogen nonbonded pair orbital (HOMO) to the LUMO+9 (flanking ring π^* ligand orbital) (Figure 4a). This high-energy absorption is also seen in complex **2** (Table 4). The energy difference between the experimental and the theoretically calculated value is 0.16 eV or 1290 cm^{-1}. A weaker absorption was calculated to appear at 454 nm and corresponds to transitions involving the HOMO (nonbonded nitrogen lone pair) to the LUMO (empty $d_{x^2-y^2}$) and LUMO+1 (empty d_{xz}) (Figure 4a). The experimentally observed transition differs by 0.24 eV or 1936 cm^{-1} from its calculated value.

For complex **2**, three less intense absorption maxima were calculated. The absorption calculated at 337 nm is a transition involving the nitrogen nonbonded pair orbital and the π (aryl) ligand orbital (HOMO) to the empty π^* (aryl) ligand (LUMO+13) and the d_{xy} orbital (SOMO 1) to the empty π^* (aryl) ligand (LUMO+2) (Figure 4b). The experimentally observed transition is only 0.05 eV (403 cm^{-1}) different from its calculated value. The absorption at 419 nm corresponds to a transition from the d_{z^2} orbital and nitrogen nonbonded pair orbital (SOMO 3) to the empty π^* (aryl) ligand (LUMO+6). The third absorption at 497 nm is a transition from the d_z^2 orbital (SOMO 3) to an empty π^* (aryl) ligand orbital and the empty $d_{x^2-y^2}$ orbital (LUMO+2). Overall the data in Table 4 represent good agreement between the calculated and experimental spectra.

Infrared Spectroscopy. Infrared spectra were recorded as Nujol mulls between CsI plates for compounds **1** and **2** and KBr for compound **3** on a Perkin-Elmer 1430 infrared spectrometer. All spectra displayed two N−H absorptions in the range 3460−3485 cm^{-1} corresponding to the predicted absorption at 3517.8 cm^{-1} (Figure 5a) and 3534.9 cm^{-1} (Figure 5b). The absorption at 555 cm^{-1} for compound **1** and at 654 cm^{-1} for compound **2** can be attributed to a stretching vibration for the N−V−N unit on the basis of calculations that were performed (cf. Figure 5). Other predicted absorptions are obscured by ligand and Nujol absorptions.

Magnetic Properties. For a stable complex with idealized $D_{\infty h}$ symmetry, first-order orbital angular momentum (OAM) is predicted for the d^1, d^3, d^6, and d^8 configurations owing to their degenerate ground states. Of these, only d^6 and d^8 complexes[7,12] have been investigated so far because stable two-coordinate complexes with d^1 or d^3 configurations (Figure 6) were unknown until now.[2]

Complex **1** displayed a predicted Curie behavior between temperatures 2 and 300 K, with slight deviation from linearity indicative of trace impurities, as seen in Figure 7a. The corresponding effective magnetic moment for $V\{N(H)Ar^{iPr_6}\}_2$ was 3.41 μ_B (Figure 7b) and is decreased from the spin-only predicted value of 3.87 μ_B. Since high-spin vanadium(II) has three unpaired electrons, there is a single d electron in the d_{xz}, d_{yz} of the degenerate orbital set which is expected to circulate freely (Figure 6).

Since a d^3 ion has a less than half-filled d shell the spin−orbit coupling parameter is positive, which leads to a magnetic moment that is lower than the spin-only value, consistent with the observed value of 3.41 μ_B.[10] If the spin−orbit contributions were fully manifested, a μ_B value of only 0.77 is predicted for

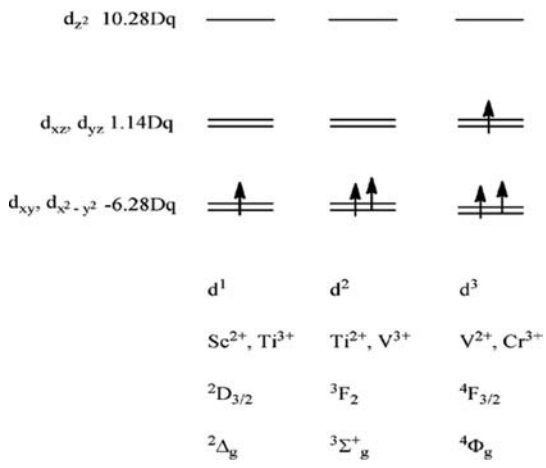

Figure 6. d^1−d^3 d-orbital splitting and ground states in a simple linear crystal field.[4]

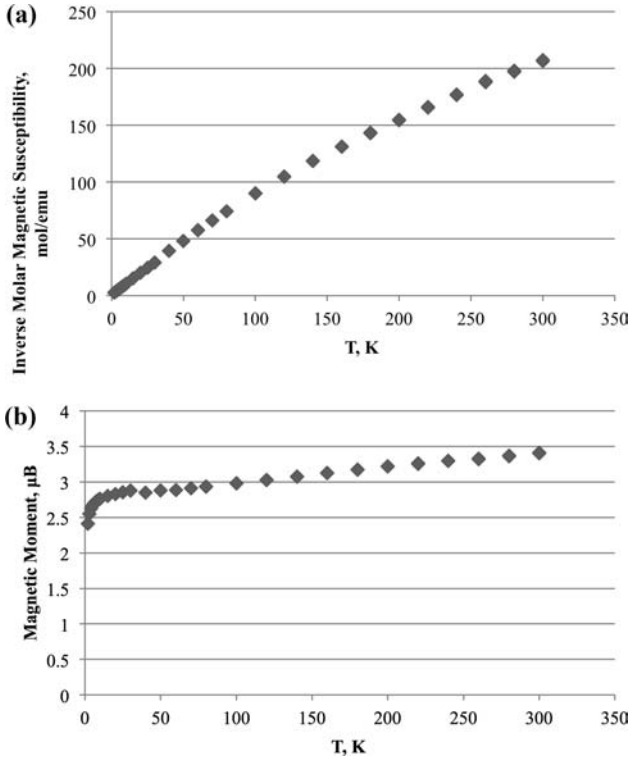

Figure 7. (a) Inverse molar susceptibility vs T plot and (b) μ_{EFF} vs T plot for the linear vanadium complex $V\{N(H)Ar^{iPr_6}\}_2$ (**1**), H(DC) = 100 Oe.

$g(J(J+1))^{1/2}$.[10,41] The fact that the observed moment is 3.41 μ_B suggests that the orbital moment is only partially quenched. This is possibly a result of metal to ligand π-bonding similar to that proposed for $Ni\{N(H)Ar^{iPr_6}\}_2$ involving the nitrogen lone pairs and the d_{xz} or d_{yz} orbitals, which interfere with electron circulation.

Complex **2** also displayed a predicted Curie behavior between temperatures 2 and 300 K, with very little deviation from linearity (Figure 8a). The corresponding effective magnetic moment for $V\{N(H)Ar^{iPr_6}\}_2$ was 2.77 μ_B (Figure 8b) at ambient temperature. This magnetic moment deviates to an even greater extent from the spin-only predicted value of 3.87 μ_B. In this respect we note that the bent structure has two vanadium sites, with 80% and 20% occupancies. For the lowest occupancy site the vanadium interacts strongly with a flanking aryl ring and has short V−C

dx.doi.org/10.1021/ja403244w | J. Am. Chem. Soc. 2013, 135, 10720−10728

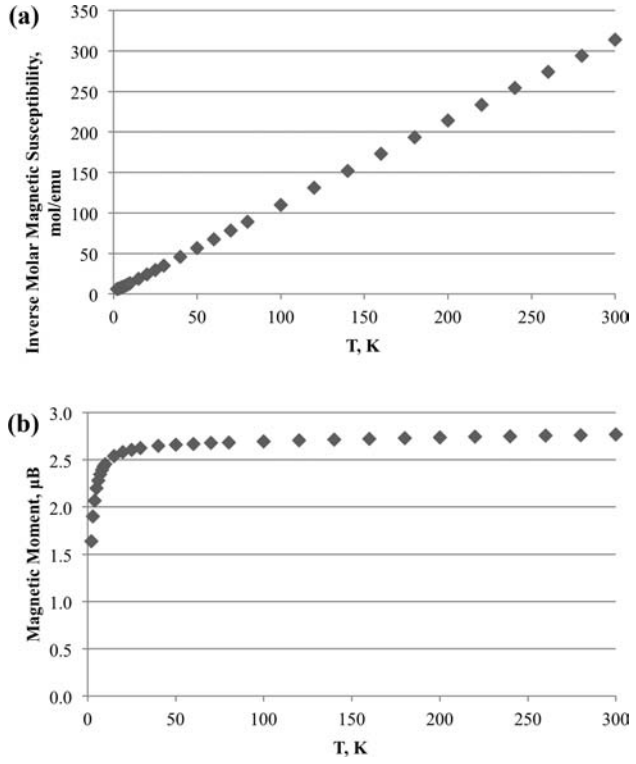

Figure 8. (a) Inverse molar susceptibility vs T plot and (b) μ_{EFF} vs T plot for the bent vanadium complex V{N(H)Ar^{Me_6}}$_2$ (**1**), H(DC) = 100 Oe.

distances consistent with V−C bond formation. In a low-spin configuration with $S = {}^1/_2$, this would cause 20% of the magnetic moment to be lower and would explain the lower overall magnetic moment. This rationalization depends on the fact that the structure is representative of the sample as a whole. In this regard, we had originally obtained a poorer-quality structure of **2**, which had a large R value. However, it displayed no disorder of the metal sites. An alternative explanation for the magnetic behavior is that both bent geometry structures are high-spin ($S = {}^3/_2$) in a C_{2v} ligand field in which two or more of the metals are approximately degenerate, thereby permitting a large orbital magnetism and hence a lower overall magnetic moment.

CONCLUSIONS

In summary, the first stable examples of two two-coordinate vanadium complexes have been synthesized and characterized. They feature linear or bent coordination at vanadium. Two synthetic approaches involving V(II) and V(III) halide precursor salts were used which afforded the amido products in reproducible yields. The linear coordination in **1** is maintained by the large size of the Ar^{iPr_6} substituents, whereas deviation of the N−V−N angle from linearity in **2** is probably due to dipolar interactions between the metal ion and the electron density of the flanking aryl rings. We have also shown that magnetic moments of the complexes are less than their spin-only values as a result of the positive spin−orbit coupling constant, although ligand−metal π bonding appears to quench the orbital contribution considerably. Work designed to synthesize two-coordinate, stable, d^1 and d^2 metal complexes is in hand.

ASSOCIATED CONTENT

Supporting Information

CIF files for the X-ray structures of **1**−**3** along with additional crystal structures, refinement methods, UV−visible spectra, and magnetic measurements. This material is available free of charge via the Internet at http://pubs.acs.org.

AUTHOR INFORMATION

Corresponding Author

pppower@ucdavis.edu.

Notes

The authors declare no competing financial interest.

ACKNOWLEDGMENTS

We thank the National Science Foundation (CHE-0948417) and a Grant-in-Aid for Specially Promoted Research (Grant no. 22000009) from MEXT of Japan for financial support and for the dual source X-ray diffractometer (Grant 0840444). We also thank Peter Klavins for assistance in the magnetization measurements.

REFERENCES

(1) Eaborn, C.; Hitchcock, P. B.; Smith, J. D.; Sullivan, A. C. *J. Chem. Soc. Chem. Commun.* **1985**, 534.
(2) Power, P. P. *Chem. Rev.* **2012**, *112*, 3482.
(3) Kays, D. L. *Dalton Trans.* **2011**, *40*, 769.
(4) Krishnam., R.; Schaap, W. B. *J. Chem. Educ.* **1969**, *46*, 799.
(5) (a) Reiff, W. M.; La Pointe, A. M.; Witten, E. H. *J. Am. Chem. Soc.* **2004**, *126*, 10206. (b) Viefhaus, T.; Schwartz, W.; Hübler, K.; Locke, K.; Weidlein, J. *Z. Anorg. Allg. Chem.* **2001**, *627*, 715. (c) LaPointe, A. M. *Inorg. Chim. Acta* **2003**, *345*, 359.
(6) Alexander Merrill, W.; Stich, T. A.; Brynda, M.; Yeagle, G. J.; Fettinger, J. C.; De Hont, R.; Reiff, W. M.; Schulz, C. E.; Britt, R. D.; Power, P. P. *J. Am. Chem. Soc.* **2009**, *131*, 12693.
(7) Stoian, S. A.; Yu, Y.; Smith, J. M.; Holland, P. L.; Bominaar, E. L.; Munck, E. *Inorg. Chem.* **2005**, *44*, 4915.
(8) (a) Sulway, S. A.; Collison, D.; McDouall, J. J. W.; Tuna, F.; Layfield, R. A. *Inorg. Chem.* **2011**, *50*, 2521. (b) Layfield, R. A.; McDouall, J. J. W.; Scheer, M.; Schwarzmaier, C.; Tuna, F. *Chem. Commun. (Cambridge, U. K.)* **2011**, *47*, 10623.
(9) (a) Cummins, C. C. *Prog. Inorg. Chem.* **1998**, *47*, 685. (b) Holland, P. L. *Acc. Chem. Res.* **2008**, *41*, 905.
(10) Figgis, B. N. *Introduction to Ligand Fields*. Wiley-Interscience: New York, 1966.
(11) Bryan, A. M.; Merrill, W. A.; Reiff, W. M.; Fettinger, J. C.; Power, P. P. *Inorg. Chem.* **2012**, *51*, 3366.
(12) Boas, L. V.; Pessoa, J. C. *Comprehensive Coordination Chemistry*; Elsevier: Amsterdam, 1987; Vol. 3, p 453.
(13) (a) Crans, D. C.; Smee, J. J. *Comprehensive Coordination Chemistry II*; Elsevier: Amsterdam, 2003; Vol. 4; (b) Song, J. I.; Berno, P.; Gambarotta, S. *J. Am. Chem. Soc.* **1994**, *116*, 6927. (c) Berno, P.; Hao, S. K.; Minhas, R.; Gambarotta, S. *J. Am. Chem. Soc.* **1994**, *116*, 7417. (d) Berno, P.; Gambarotta, S. *Angew. Chem., Int. Ed.* **1995**, *34*, 822.
(14) Pangborn, A. B.; Giardello, M. A.; Grubbs, R. H.; Rosen, R. K.; Timmers, F. J. *Organometallics* **1996**, *15*, 1518.
(15) Tilley, T. D.; Gavenonis, J. *Organometallics* **2000**, *21*, 5549.
(16) Twamley, B.; Hwang, C. S.; Hardman, N. J.; Power, P. P. *J. Organomet. Chem.* **2000**, *609*, 152.
(17) Kiesel, R.; Schram, E. P. *Inorg. Chem.* **1973**, *12*, 1090.
(18) Hope, H. *Prog. Inorg. Chem.* **1995**, *41*, 1.
(19) (a) Blessing, R. H. *Acta Crystallogr.* **1995**, *A51*, 33. (b) Sheldrick, G. M. *SADABS, Siemens Area Detector Absorption Correction*; 2008.
(20) (a) Sheldrick, G. M. *SHELXTL*; 2002. (b) Sheldrick, G. M. *SHELXS97 and SHELXL97*; 1997.
(21) Bain, G. A.; Berry, J. F. *J. Chem. Educ.* **2008**, *85*, 532.
(22) Frisch, M. J. *Gaussian 09, Revision A.01*, Gaussian, Inc.: Wallingford, CT, 2009.
(23) (a) Becke, A. D. *Phys. Rev. A* **1988**, *38*, 3098. (b) Becke, A. D. *J. Chem. Phys.* **1993**, *98*, 5648.
(24) Perdew, J. P.; Wang, Y. *Phys. Rev. B* **1992**, *45*, 13244.

(25) Manzer, L. E. *Inorg. Synth.* **1982**, *21*, 138.
(26) (a) Bradley, D. C.; Copperthwaite, R. G. *Inorg. Synth.* **1978**, *18*, 116. (b) Sutton, A. D.; Fettinger, J. C.; Rekken, B. D.; Power, P. P. *Polyhedron.* **2008**, *27*, 2515.
(27) Andersen, R. A.; Faegri, K.; Green, J. C.; Haaland, A.; Lappert, M. F.; Leung, W. P.; Rypdal, K. *Inorg. Chem.* **1988**, *27*, 1782.
(28) Bradley, D. C.; Copperthwaite, R. G. *Inorg. Synth.* **1978**, *18*, 117.
(29) (a) Lappert, M. F.; Protchenko, A.; Power, P. P.; Seeber, A. *Metal Amide Chemistry*; John Wiley & Sons: 2008; p 370. (b) Evans, D. J.; Hughes, D. L.; Silver, J. *Inorg. Chem.* **1997**, *36*, 747. (c) MacDonnell, F. M.; Ruhland-Senge, K.; Ellison, J. J.; Holm, R. H.; Power, P. P. *Inorg. Chem.* **1995**, *34*, 1815.
(30) (a) Shannon, R. D.; Prewitt, C. T. *Acta Crystallogr.* **1969**, *B25*, 925−946. (b) Boynton, J. N.; Merrill, W. A.; Fettinger, J. C.; Reiff, W. M.; Power, P. P. *Inorg. Chem.* **2012**, *51*, 3212.
(31) Tran, B. L.; Pintér, B.; Nichols, A. J.; Konopka, F. T.; Thompson, R.; Chen, C.-H.; Krzystek, J.; Ozarowski, A.; Telser, J.; Baik, M.-H.; Meyer, K.; Mindiola, D. J. *J. Am. Chem. Soc.* **2012**, *134*, 13035.
(32) (a) Pyykko, P.; Atsumi, M. *Chem.—Eur. J.* **2009**, *15*, 186. (b) Lorber, C. *Comprehensive Organometallic Chemistry III*; Crabtree, R. H., Mingos, D. M. P., Theopold, K. H., Eds.; Elsevier: Oxford, 2007; Vol. 5, Chapter 5.01.
(33) (a) Bocarsly, J. R.; Floriani, C.; Chiesi-Villa, A.; Guastini, C. *Inorg. Chem.* **1987**, *26*, 1871. (b) Chang, K.-C.; Lu, C.-F.; Wang, P.-Y.; Lu, D.-Y.; Chen, H.-Z.; Kuo, T.-S.; Tsai, Y.-C. *Dalton Trans.* **2011**, *40*, 2324.
(34) Mulvey, R. E. *Chem. Soc. Rev.* **1991**, *20*, 167.
(35) (a) Wells, A. F. *Structural Inorganic Chemistry*, 6th ed.; Clarendon: Oxford, 1984; p 1195. (b) Butler, A.; Clague, M. J.; Meister, G. E. *Chem. Rev.* **1994**, *94*, 625.
(36) (a) Nakajima, K.; Tokida, N.; Kojima, M.; Fujita, J. *Bull. Chem. Soc. Jpn.* **1992**, *65*, 1725. (b) Mandal, T. N.; Roy, S.; Gupta, S.; Paul, B. K.; Butcher, R. J.; Rheingold, A. L.; Kar, S. K. *Polyhedron* **2011**, *30*, 1595.
(37) Berno, P.; Minhas, R.; Hao, S. K.; Gambarotta, S. *Organometallics* **1994**, *13*, 1052.
(38) (a) Cozzolino, A. F.; Tofan, D.; Cummins, C. C.; Temprado, M.; Palluccio, T. D.; Rybak-Akimova, E. V.; Majumdar, S.; Cai, X. C.; Captain, B.; Hoff, C. D. *J. Am. Chem. Soc.* **2012**, *134*, 18249. (b) Tran, B. L.; Chen, C. H.; Mindiola, D. J. *Inorg. Chim. Acta* **2011**, *369*, 215.
(39) Stanciu, C.; Olmstead, M. M.; Phillips, A. D.; Stender, M.; Power, P. P. *Eur. J. Inorg. Chem.* **2003**, 3495.
(40) (a) Diedrich, F.; Klingebiel, U.; Schafer, M. *J. Organomet. Chem.* **1999**, *588*, 242. (b) Fernandez, I.; Price, R. D.; Bolton, P. D.; Mahon, M. F.; Davidson, M. G.; Lopez-Ortiz, F. *J. Organomet. Chem.* **2004**, *689*, 1890. (c) Cetinkaya, B.; Gumrukcu, I.; Lappert, M. F.; Atwood, J. L.; Shakir, R. *J. Am. Chem. Soc.* **1980**, *102*, 2086. (d) Hvoslef, J.; Hope, H.; Murray, B. D.; Power, P. P. *J. Chem. Soc. Chem. Commun.* **1983**, 1438. (e) Huffman, J. C.; Geerts, R. L.; Caulton, K. G. *J. Crystallogr. Spectrosc. Res.* **1984**, *14*, 541. (f) Thiele, K.; Gorls, H.; Imhof, W.; Seidel, W. *Z. Anorg. Allg. Chem.* **2002**, *628*, 107. (g) Pauer, F.; Power, P. P. *Lithium Chemistry, A Theoretical and Experimental Overview*; Sapse, A.-M., Schleyer, P. v. R., Eds.; Wiley: New York, 1995; Chapter 9.
(41) Drago, R. S. *Physical Methods for Chemists*, 2nd ed.; Harcourt Brace Jovanovich: New York, 1992; p 484.